Natural Computing
https://doi.org/10.1007/s11047-023-09962-1

Synchronization of elementary cellular automata

Théo Plénet[1] · Franco Bagnoli[3] · Samira El Yacoubi[1] · Clément Raïevsky[2] · Laurent Lefèvre[2]

Accepted: 1 August 2023

Abstract
In this paper, we study how synchronization and state estimation are related in the context of elementary cellular automata. We first characterize the geometric properties of the synchronization error between two replicas of a 1D elementary cellular automata following Wolfram's rule 18. We propose a simple approach to statistically model the transient phase of the spreading of the synchronization error. We finally present a way to utilize our model of the error spreading to place mobile sensors in order to improve the overall replica synchronization in the case in which the initial error is small.

Keywords Cellular automata · Synchronization · Observation · Mobile sensors

1 Introduction

In control theory, the process of monitoring physical systems which are distributed in space is based on the construction of a state estimate from measurements and the dynamics of the system. The measurements can potentially come from mobile sensors. The problem of positioning these sensors is crucial to make the estimate the state of the system possible. This state estimation problem is widely studied by classical control theory (Kalman 1963; Sarachik and Kreindler 1965) and it follows from the verification of observability, a notion that ensures that the sensors are well placed. This notion of observability can be applied to cellular automata (CA) (El Yacoubi et al. 2021; Plénet et al. 2022; Dridi et al. 2019) (and by extension to Boolean networks Zhu et al. (2018), which can be seen as a generalization of CA) but its evaluation has proven to be extremely complicated when one deals with non-linear CA Plénet et al. (2022).

In this paper we apply the concept of master–slave or drive-response synchronization Pecora and Carroll (1990, 2015) to the problem of controlling cellular automata. The master–slave synchronization problem consists in studying two replicas of a system, which evolve following the same rule but starting from different initial conditions. One of these replicas is the master, which can also be thought as the "real" or experimental system upon which local observations are made. The goal is to have the slave replica, which in general is simulated on a computer, synchronized with the master. In this way, one can use the replica to perform measurements which are impossible to be performed on the master system, or as a way of forecasting the master's future dynamics. This approach is most interesting when the dynamics of the system is chaotic, so that they never synchronize spontaneously, i.e., the difference in their states (error) remains always finite. The master–slave synchronization consists in imposing the state of local variables objects of measurements to the corresponding state variables of the slave system, i.e., establishing a unidirectional local coupling between the two replicas.

In the case of CA, the state of some cells of the master replica are copied to these same cells of the slave one. The

✉ Laurent Lefèvre
laurent.lefevre@lcis.grenoble-inp.fr

Théo Plénet
theo.plenet@univ-perp.fr

Franco Bagnoli
franco.bagnoli@unifi.it

Samira El Yacoubi
yacoubi@univ-perp.fr

Clément Raïevsky
clement.raievsky@lcis.grenoble-inp.fr

[1] UMR Espace-Dev, University of Perpignan Via Domitia, Perpignan, France

[2] LCIS, Univ. Grenoble Alpes, Grenoble INP, Valence, France

[3] Physics and Astronomy and CSDC, University of Florence, Florence, Italy

Published online: 25 August 2023

coupling between the two replicas can be implemented on a a single cell Dogaru et al. (2009), on a fixed set of cells Urıas et al. (1998), or on randomly chosen cells at each time step Bagnoli and Rechtman (1999). In the first case, Dogaru et al. showed that a strong condition regarding the chaoticity of the system is needed to synchronize the driver and the replica. In the second case, Urías et al. proposed a necessary and sufficient condition concerning the cell position to ensure the synchronization of linear elementary cellular automata. Finally, Bagnoli and Rechtman proposed a statistical approach to synchronization, defining a critical probability $p > p_c$ that ensures synchronization. The problem of synchronization of two CA can also be seen as a state estimation problem. Indeed, the driver can be seen as the system to be observed, the replica as the state estimator and the synchronized cells as sensors. For the purpose of monitoring physical systems, the conditions on the system imposed by Dogaru et al. (choaticity) and by Urías et al. (linearity) make it difficult to apply their schemes to this type of system. The approach of Bagnoli and Rechtman, on the contrary, is not based on a specific type of system. Moreover, it allows to include the notion of mobile sensor on choice of synchronized cells, which can be random, as in the original paper, or targeted based on error measurement, as done for intance in Ref Bagnoli and Rechtman (2018) for probabilistic cellular automata.

The main objective of this paper is to exploit the synchronizion of CA as a state estimator for the observation of distributed parameter system with spatio-temporal dynamics. We focus on synchronization with a small initial error because in some physical system monitoring, only a small portion of the system is unknown. For example, when monitoring the spreading of forest fires, the topology of the forest is known but the ignition points are unknown. Throughout this article, we focus on a single elementary rule that exhibits spatio-temporal dynamics so that the obtained results may be transferred to other CA and in particular to physical systems. Therefore, we chose to study the elementary rule 18 because it is the smallest chaotic, symmetric, and nonlinear rule Wolfram (1984).

In Sect. 2 we start by studying the differences in synchronization performances as a function of the initial synchronization error. Then, in Sect. 3, we model the spreading of the initial error within the CA using basic geometry. We proceed by presenting an improvement of the synchronization algorithm for systems with a small initial error in Sect. 4. Finally, an application to mobile detectors is presented in Sect. 5. Conclusions are drawn in the last section.

2 Influence of initial error on synchronization

In order to study the impact of the initial error on the synchronization performance, we need to define the synchronization method but also to express it in terms of the initial error. For this purpose, we chose the definition proposed by Bagnoli and Rechtman (1999) which expresses the synchronization of two 1D CA of N cells: the driver x and the replica y. The synchronization of y with x is done by copying the state of some cells of x in the matching cells in y, at each time step. The diagonal matrix P indicates which cells of the CA are coupled. A value of 1 in this matrix indicates that the corresponding cells are coupled. The state variables evolve as:

$$\begin{cases} x_{t+1} = f(x_t), \\ y_{t+1} = (I - P) \cdot f(y_t) \oplus P \cdot f(x_t), \end{cases} \tag{1}$$

where $\oplus$ indicates the sum modulo two (exclusive or), to be performed cell by cell.

The synchronization error e_t is the difference between x_t and y_t, and ϵ_t the normalized mean value of e_t. Since we are studying the influence of the initial error, we initialize x_0 and e_0 randomly and set $y_0 = x_0 \oplus e_0$. We denote by e the proportion of cells in y_0 that are different from cells in x_0, in percentage:

$$\begin{cases} e_t = x_t \oplus y_t \\ \epsilon_t = \dfrac{1}{N} \cdot \sum_i e_t^{(i)} \end{cases} \tag{2}$$

The position of the coupled cells are determined randomly at each time step with a probability p, called the control strength. In Bagnoli and Rechtman (1999), Bagnoli and Rechtman discuss the notion of critical control strength p_c (determined statistically or estimated analytically using the maximum Lyapunov exponent), which guarantees that the asymptotic synchronization is complete employing a random synchronization.

This critical parameter ensures, for a state estimator, that the estimated state correctly corresponds to the state of the observed system, after a long enough time T. In Sect. 4, we present an improvement of this synchronization algorithm in order to reduce the critical control strength needed for synchronization.

To better visualize the impact of control strength on synchronization performance, we present on Fig. 1a the mean synchronization error and the synchronization rate as a function of control strength for $T = 750$. On Fig. 1b we represent the mean synchronization time necessary to

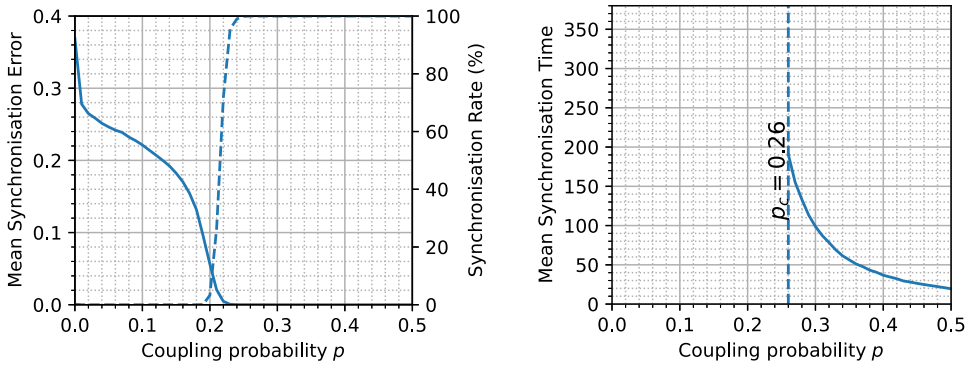

(a) synchronization error (continuous) and rate (dashed)

(b) Mean synchronization time

Fig. 1 Evolution of the synchronization error, rate and time, as a function of control strength p for the elementary CA rule 18 with 500 cells

synchronize the replica on the driver. The critical control strength at which the slave replica synchronizes in all cases is $p_c = 0.26$. Starting from this value, the slave replica asymptotically synchronizes with the driver. If the control strength is increased, the time required to reach synchronization decreases.

Figure 2 shows the mean synchronization error ϵ_t as a function of time for different values of the initial error ϵ_0. These results were obtained by taking the mean of the synchronization error ϵ_t over 500 simulations for the elementary rule 18 with 500 cells and a control strength $p = 0.1$. The initial configuration x_0 was randomly initialized at each simulation, the same for the initialy unsynchronized cells in the replica y_0.

The size of the initial error has a clear impact on the performances of synchronization. Its first influence is on the speed of convergence towards the asymptote. Indeed, the 10% curve seems to converge faster than the 20% and 100% curves which converges earlier than the 1% and 0.2% curves. The second effect of the initial error is on the value of the asymptote when the error is small enough. For sufficiently large errors, all simulations converge towards the same asymptote value, around 0.23. But if ϵ_0 is sufficiently small, the reached asymptote is lower than this "generic" one.

To understand the difference in value between the two asymptotes, we studied the evolution of the error as a function of time for the particular case of a single cell of initial error ($e_0 = 0.2\%$). As we can see on Fig. 3, there are two very different kinds of evolution of the synchronization error e_t. On one hand, in Fig. 3a, the error spreads until it covers the whole CA and reaches the asymptotic non-zero value. On the other hand, in the very specific case depicted on Fig. 3b, the synchronization quickly becomes total and the error reaches zero. Therefore, when we average these two cases, which we did for Fig. 2, we obtain a lower asymptotic value than the generic case will give. For the remaining of the study, we chose to dissociate the two cases and to not consider the quick total synchronization cases when we study the asymptotic value.

To characterize the influence of the initial error ϵ_0 on the ability of the synchronized CA to be considered as a state estimate, we will only consider the mean of the asymptotic value of the synchronization error. Figure 4 represents this mean asymptotic synchronization error as a function of the initial error. First, if we consider only the asymptotic

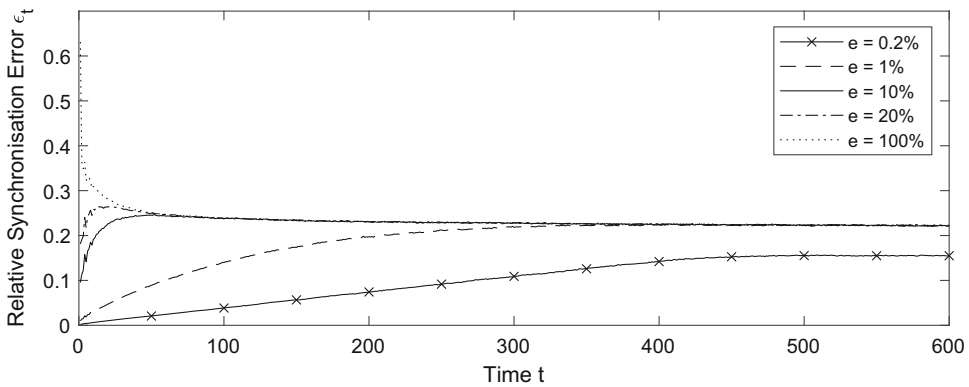

Fig. 2 Mean synchronization error as a function of time for different initial error ϵ_0

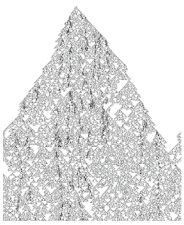

(a) Asymptotic Synchronization (b) Total Synchronization

Fig. 3 Evolution of the synchronization error for elementary rule 18 with 500 cells from a single cell error ($e_0 = 0.2\%$). The time is represented on the vertical axis. A black pixel is an erroneous cell in the synchronized CA

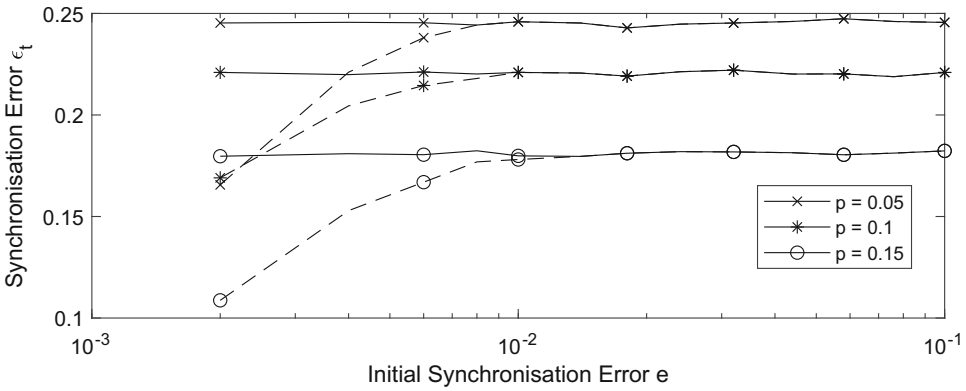

Fig. 4 The asymptotic value of the mean synchronization error as a function of initial error ϵ_0. This was obtained by taking the mean of the synchronization error ϵ_t as a function of time over 200 iterations. The continuous lines consider only the asymptotic synchronization while the dashed lines include both asymptotic and early total synchronization

synchronization (without special cases of early complete synchronization), the value of the asymptote does not depend on the initial error. Secondly, the value from which the mean error with and without total synchronization becomes different depends on the strength of the control p: the stronger the control, the larger the chances of total synchronization.

3 Modeling of the error spreading dynamics

In order to explain the dynamics of the evolution of the synchronization error, we will study how the error propagates within the CA as a function of the control strength. To do so, we will start by studying the propagation of the error with the simple case of a single erroneous cell, and then generalize these results.

Typical error propagation dynamics from one erroneous cell are depicted in Fig. 5. Clearly, the propagation is limited by the "propagation cone" (triangle in 1D) of defects: since the future value of a cell depends on that of first neighbors, a defect can at most spread one cell at left and right at a time, thus the "speed of light" is one for elementary CA. We therefore adopted the triangle as a simple geometric model for these dynamics. It appears that the top angle of the triangle is inversely proportional to the control strength p.

To describe how the synchronization error spreads, two parameters will be used: the first being the aperture angle of the propagation triangle, and the second being the shift angle between the altitude and the median of the triangle. Indeed, the median of the triangle seems to vary from one simulation to another. Figure 6 describes the geometry associated with these angles α and β which describe respectively the aperture angle and the shift angle.

For the purpose of this article, we will not use directly the α and β angles but their tangents, which represents spread velocities and drifts (shift). We will simply call α and β the velocities associated to the angles and not the angles themselves. Therefore, the **error spreading ratio** α represents the mean number of cells by which the triangle base increases at each time step and **error shift ratio** β the mean number of cell shift at each time step.

(a) $p = 0.0$ (b) $p = 0.05$ (c) $p = 0.10$ (d) $p = 0.15$

Fig. 5 Evolution of the error for elementary rule 18 with 500 cells from a single erroneous cell ($e = 0.2\%$). The time is represented on the vertical axis

We can calculate the mean value of the error spreading ratio by measuring the area of the error at time T and divide by current time to obtain the tangent of α. Figure 7 describes the evolution of the mean spreading ratio as a function of the control strength. This one is a linear function of which we numerically obtained the relation $\alpha = -8.23.p + 1.93$ using linear regression.

The error spreading ratio α has, for a given control strength, a normal distribution whose mean is presented on Fig. 7. The standard deviation related to α can be calculated in order to have a better representation of α. The error shift ratio β also follows a normal distribution. Based on these two parameters, we can express the width and the center of the error at time T by $c_1 = c_0 + \beta \cdot T$ and $d = \alpha \cdot T$.

Proposition 1 *The synchronization error ϵ_T can be estimated from the parameter α as well as the value of the asymptote γ associated to the control strength p. Thus, the synchronization error ϵ_T is defined by*

$$\epsilon_T = \frac{\gamma}{N} \cdot \max(\alpha \cdot T, N)$$

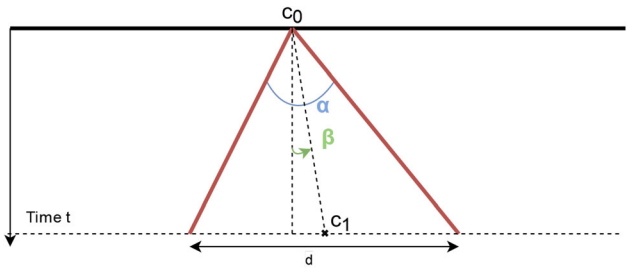

Fig. 6 Schematic of the theoretical spread of the synchronization error from a single initial error cell

Indeed, $\alpha \cdot T$ gives the width of the error in number of cells. By dividing it by N, we obtain the normalized error width and then multiplying by the asymptote γ, the value of ϵ_t when the error occurs on the whole CA, we obtain the synchronization error ϵ_T.

Using the Proposition 1, we can make an example for $p = 0.1$. For this control strength, the error spreading ratio α follows a normal distribution with mean 1.127 and standard deviation 0.1376. On Fig. 8, the synchronization error ϵ_T is displayed as well as the estimated error with an α fixed at the mean, and an α following the normal distribution. We quickly notice that the use of the normal distribution in the calculation of the error allows to explain the rounded curve when the error approaches the asymptote. However, the two theoretical curves have a difference with the real curve which is explained by a faster increase of the error during the first iterations which is caused by a higher α as the error is not yet detected, and therefore controlled, by the sensor.

This method allows us to simply represent the propagation of the error in the case where a single cell is erroneous in the initial configuration. If we consider two or more erroneous cells then the modeling becomes more complex. Indeed, the two errors propagate independently until they *collide*, in this case we must consider that the errors merge in a single (larger) source of error. Thus, considering that the collision takes place at time t_1, we can consider that the error spreading ratio α is expressed as

$$\alpha(t) = \begin{cases} \alpha_0 + \alpha_1 & \text{if } t \leq t_1; \\ \dfrac{(\alpha_0 - \beta_0 + \alpha_1 + \beta_1)}{2} & \text{if } t \geq t_1. \end{cases}$$

The time t_1 of the collision depends on the initial distance between the two initial errors, whose probability distribution depends on the boundary conditions used. Moreover,

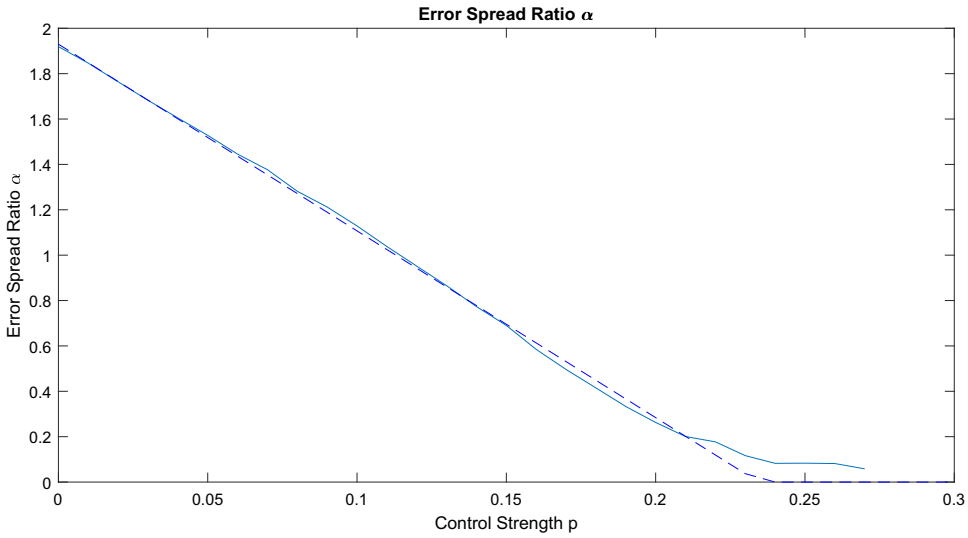

Fig. 7 The error propagation coefficient α as a function of control strength. The continuous curve is obtained by taking the mean of α over 1000 simulations. The dashed curve is the curve obtained by linear regression

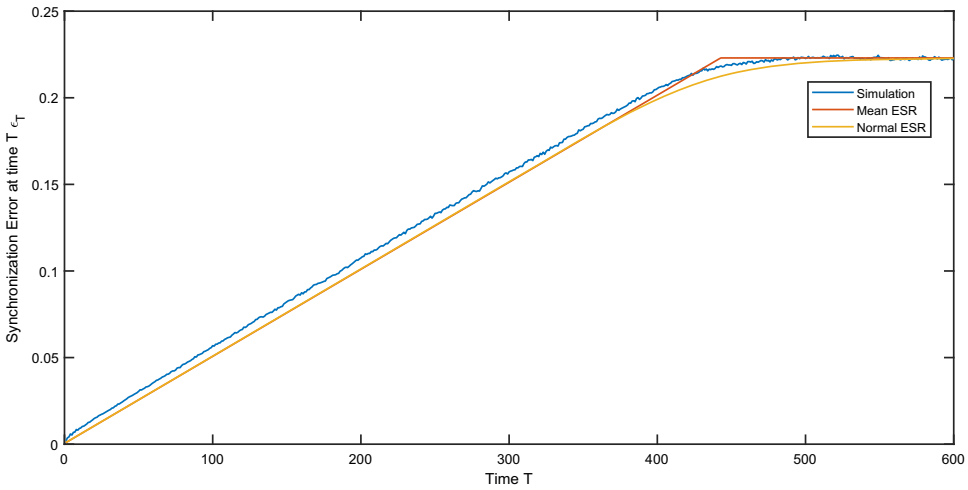

Fig. 8 Evolution of the mean synchronization error as a function of time for the real case as well as the theoretical cases with the error spreading ratio which is constant and follows a normal distribution

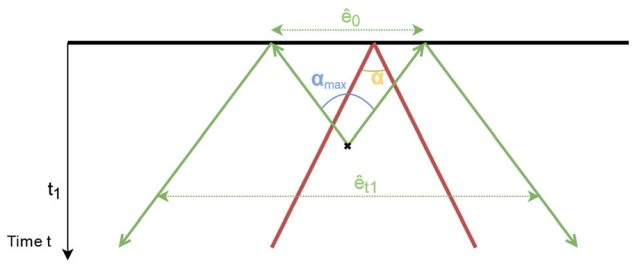

Fig. 9 Schematic of the backpropagation of the synchronization error to find the initial error area $\hat{e}_0$

since each of these initial errors is subject to the total and quick synchronization (probability τ), the model must include, with probability $2\tau(1-\tau)$, a propagation with only one initial error, as illustrated in Fig. 6. With more than two erroneous cells, the operation is the same but it is necessary to take into account several collisions at different times.

4 Optimization of algorithm for a single erroneous cell

If we consider that the synchronized cellular automaton has only a few errors at initialization, then it is possible to adapt the synchronization algorithm so as to concentrate the sensors only on the area that contains errors. To do this, we must first identify the areas that possibly contain errors and then distribute the sensors over those.

To identify the error area, a sensor must fisrt detect an error. Then, with a method similar to the one shown in Fig. 6, it is possible to backpropagate the error measured at time t to obtain the possible error area $\hat{e}_0$ at time 0 which could lead to the initial error. Propagating an error from this initial estimate, we can obtain the possible current error area $\hat{e}_t$. Figure 9 represents the backpropagation of the error with a ratio α_{max} which corresponds to a ratio α large enough to include all (or a large part) of the possible spread ratios. The maximum ratio is 2 because it is not possible for the error to spread to more than one cell on each side (this results from the size of the neighbourhood) but if the strength of the control p is strong enough, α_{max} can be chosen smaller. As α follows a normal distribution, a ratio $\alpha_{max} = \alpha_{mean} + 3\sigma$ encompasses 99.9% of the possible spreading ratios.

As new errors are detected, the initial error area can be refined using the intersection of all the initial error areas of all the errors detected by the sensors. In this way, it is possible to reduce the size of the error zone at time t but also to locate the position of the initial error.

Now that error area can be estimated, it remains to position the sensors. The method consists in placing the sensors only in the area where the error could be present. The number of sensors will remain the same but the control strength (the sensor density) of the error area will increase proportionally to the smallness of the error area resulting in a lower critical control strength p_c as shown in Fig. 10. The control strength in the error area is described by:

$$p_{error} = p \cdot \frac{N}{\hat{\epsilon}_t}. \tag{3}$$

As shown in Fig. 10, the optimized synchronization performs better than the usual one with a critical control strength p_c at 0.05 instead of 0.21. However, when the control is too weak, the difference between the two is negligible because the first error cell is detected too late by the sensors and therefore the optimized control strength p_{error} is not sufficient to synchronize the two systems.

In Fig. 11, we have compared these two synchronization methods on other elementary rules belonging to different classes Wolfram (1984). The results obtained are lower bounds because the error spreading ratio used for the backpropagation is $\alpha_{max} = 2$, smaller values according to

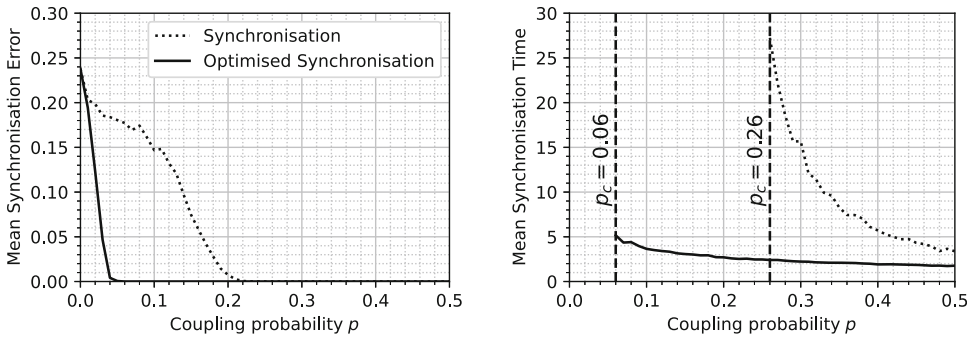

(a) Mean synchronization error (b) Mean synchronization time

Fig. 10 Evolution of the mean synchronization error (a) and time (b) as a function of control strength for a single cell error

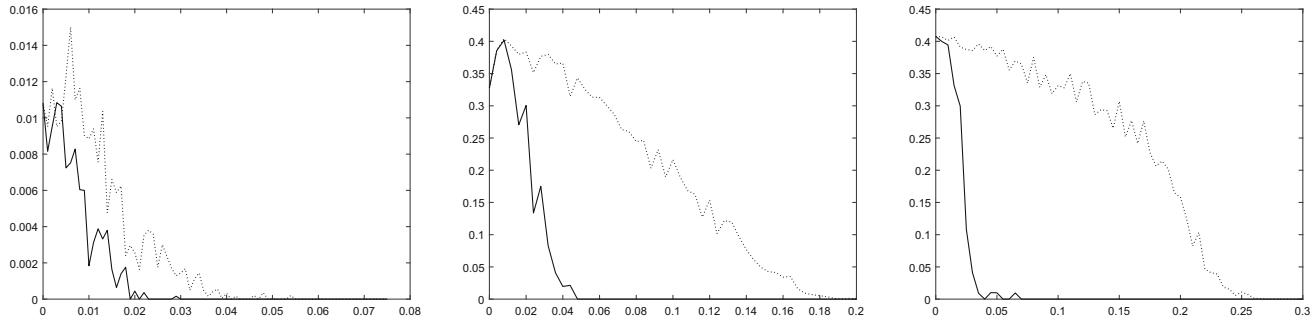

(a) rule 37 (b) rule 110 (c) rule 126

Fig. 11 Evolution of the mean synchronization error as a function of control strength p for a single cell error for different rules. From left to right: rule 37 class 2; rule 110 class 4; and rule 126 class 3. Continuous line represents the optimized synchronization and dotted line the usual synchronization

the distribution of probability could have been chosen to further increase the performances. Overall, the optimized synchronization performs better but the difference between the two seems to depend on the class. Class 2 CA (presented by Wolfram as "filters") seem to exhibit lower error propagation coefficients α than class 3 and 4 CA. Without control, α is 0.048 for rule 37, 0.54 for rule 110 and 1.9 for rule 126. However, a systematic study on elementary CA would be necessary to confirm this conjecture.

It is also important to note that the performance of this optimized synchronization method depends on the size N of the CA. Indeed, as the propagation of the initial error is independent of the CA size as long as it has not covered the whole CA, then $\hat{e}_t$ does not depend on N. Therefore, from Eq. (3), we can see that to ensure a constant p_{error} then p can decrease as N grows. However, we need a control strength p large enough to measure an error cell before the error has propagated too significantly. In Fig. 12, this effect was highlighted by comparing the synchronization performance for several CA sizes. It appears that a lower critical control strength is achieved when the size of the CA grows. This is due to the focusing of a greater number of synchronized cells on an area with a similar size.

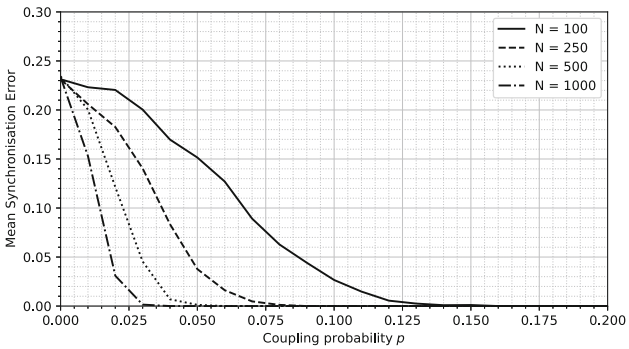

Fig. 12 Evolution of the mean synchronization error as a function of size of the CA for the optimized synchronization

5 Mobile sensors synchronization

In a context of physical system observation, random synchronization can be seen as mobile sensors that jump between each measurement point, but it is rather rare that such mobile sensors cannot measure the cells between the two positions. Therefore, we propose a new

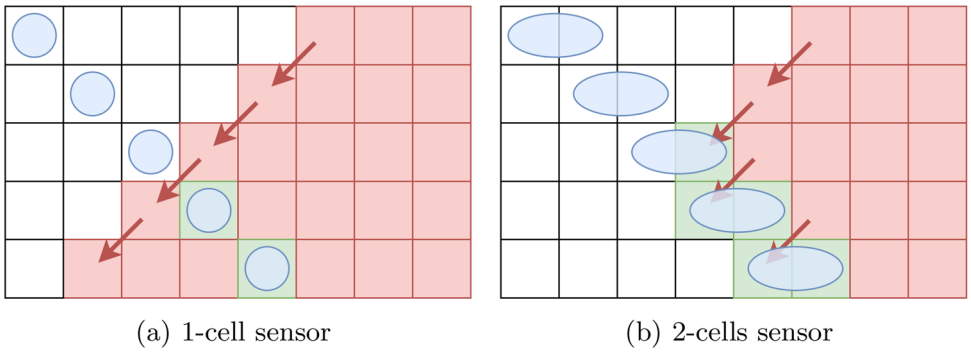

(a) 1-cell sensor (b) 2-cells sensor

Fig. 13 Example of a mobile sensor with 1 or 2 cells. The sensors are the blue ellipses, the red cells represent the error between the replica and the driver and the green cells represent the errors correctly corrected by the sensors

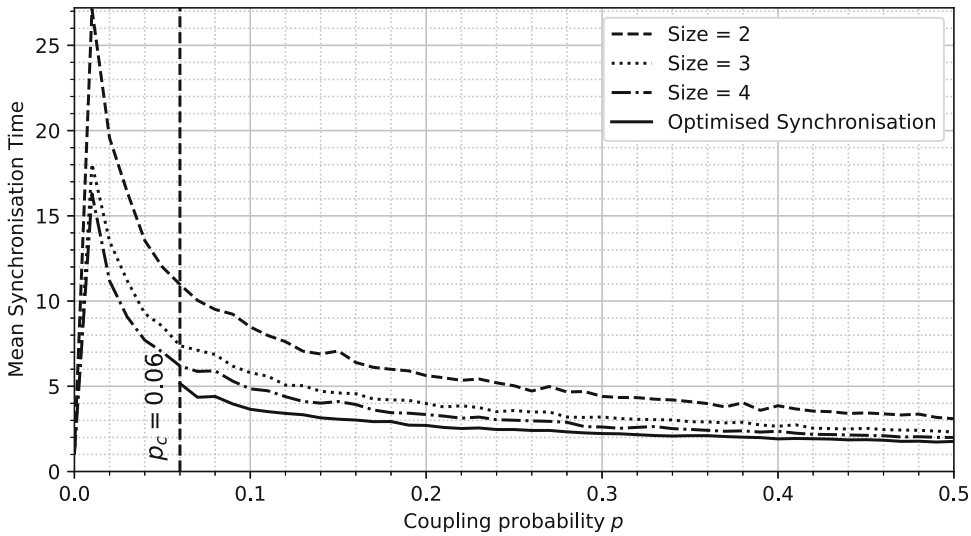

Fig. 14 Evolution of the mean synchronization error for the optimized synchronization as a function of size of the mobile sensors

synchronization method more suitable for the observation of physical system by mobile sensors.

This method is a variant of the optimized method in which once we have bounded the possible error zone $\hat{e}_t$ we place two mobile sensors at both ends of this zone. The sensors will then gradually move towards each other such that they travel across the entire error zone. The sensors must be large enough, in terms of number of measured cells, in order to act as a border for which the error cannot leave the zone without being detected by a sensor.

Indeed, as depicted in Fig. 13a, if the mobile sensor is composed of only one cell, then when moving, it may not measure enough cells to block the propagation of the synchronization error. In the case where the sensor is composed of 2 cells then the synchronization error cannot propagate beyond the sensor (see Fig. 13b). More generally, it is necessary that when the sensor moves there is a cell in common between the two positions to be sure that the propagation of the synchronization error of the first unmeasured cell is measured at the next time step. As a result, for a moving sensor composed of k cells, its moving speed must be at most $k - 1$ cells per iteration.

One of the main advantage of this synchronization method is that it is independent of the control strength. Indeed, with at least two 2-cells mobile sensors then the synchronization is ensured. Of course, if more sensor are available or if the sensors are composed of more cells, then the synchronization can be more efficient. Therefore, using the mean synchronization error as a function of the control strength is not relevant for this synchronization. Instead, we focus on the synchronization time which will be impacted by size and number of mobile sensors.

In Fig. 14, we compare the synchronization time for different sizes of sensors on the elementary rule 18 with 500 cells. The control strength has an impact on the detection of the first error cell and therefore on the time at which the error area is first determined. The sooner the detection of the error occur, the smaller the error area and the smaller the synchronization time is. The synchronization time decreases well with the increase in size, and therefore speed, of the mobile sensors. However, the gap between sizes decreases as the control strength increases. This is because the error is detected sooner and therefore the size of the error area is smaller. The optimized

synchronization performance is a lower bound for synchronization time since, for some value of the control strength, there will be as many sensors to place as cells in the error area.

In this application, the synchronization is ensured by two mechanisms: an error detection and an error synchronization. This approach leads to a method of coordination of mobile sensors. A related approach based on multi-agent systems has been discussed in Plénet et al. (2020). In this work, mobile sensors were used to monitor a 2-dimensional forest fire model with fire detection by "explorers" and fire propagation monitoring by "followers". The synchronization method we just presented is more complicated to apply to this forest fire model because the error area must be circumscribed: the error area frontier shape being dependent on the CA neighborhood, the forest fire has a square shaped limit which is way larger than the two points required for 1-dimensional CA. The number of sensors needed to ensure the synchronization in the case of 2-dimensional CA is therefore much greater than with 1-dimensional CA.

6 Conclusion and perspectives

In this paper we studied how CA synchronization relates to state estimation of distributed parameter system in the context of Wolfram's 18th rule. In order to understand how a synchronized CA can be seen as an estimated state, we studied the dynamics of the synchronization error spreading. To do so we proposed a simple geometric model of this propagation. Finally, we present a sensors placement algorithm utilizing this geometric model in order to reduce the synchronization error and improve the accuracy of the synchronized CA as an estimate of the original CA representing the studied system. This optimized synchronization has been studied in the case of different elementary rules of classes 2, 3 and 4. The measured performance increase compared to the usual synchronization is particularly important in the case of classes 3 and 4.

In the future, we plan to extend this algorithm to that case in which there is more than a single initial error cell. Furthermore, a systematic study on the elementary automata rules could be carried out in order to refine the algorithm of synchronization according to damage (error) spreading dynamics.

Author Contributions All authors contributed equally to this work and reviewed the manuscript.

Funding Théo Plenet received a funding from the University of Perpignan Via Domitia for this work (PhD grant from Doctoral School 305)

Data and materials availability source codes and numerical simulation results are available on request from the corresponding author

Declarations

Conflict of interest there is no competing interests of any financial or personal nature

Ethical approval Not applicable.

References

Bagnoli F, Rechtman R (1999) Synchronization and maximum Lyapunov exponents of cellular automata. Phys Rev E 59(2):1307. https://doi.org/10.1103/PhysRevE.59.R1307

Bagnoli F, Rechtman R (2018) Regional synchronization of a probabilistic cellular automaton. In: Cellular Automata, Proceedings of 13th International Conference on Cellular Automata for Research and Industry, ACRI 2018, Como, Italy, September 17-21, 2018; LNTCS, Vol 11115, pp. 255–263. Springer, Switzerland. https://doi.org/10.1007/978-3-319-99813-8_23

Dogaru R, Dogaru I, Kim H (2009) Binary chaos synchronization in elementary cellular automata. Int J Bifurc Chaos 19(09): 2871–2884. https://doi.org/10.1142/S0218127409024529

Dridi S, Bagnoli F, Yacoubi SE (2019) Markov chains approach for regional controllability of deterministic cellular automata, via boundary actions. J Cell Autom 14(5/6):479–498

El Yacoubi S, Plénet T, Dridi S, Bagnoli F, Lefèvre L, Raïevsky C (2021) Some control and observation issues in cellular automata. Complex Syst 30(3):391–413. https://doi.org/10.25088/ComplexSystems.30.3.391

Kalman RE (1963) Mathematical description of linear dynamical systems. J Soc Ind Appl Math, Ser A: Control 1(2):152–192. https://doi.org/10.1137/0301010

Pecora LM, Carroll TL (1990) Synchronization in chaotic systems. Phys Rev Lett 64(8):821–824. https://doi.org/10.1103/physrevlett.64.821

Pecora LM, Carroll TL (2015) Synchronization of chaotic systems. Chaos: Interdiscip J Nonlinear Sci 25(9):097611. https://doi.org/10.1063/1.4917383

Plénet T, Raïevsky C, Lefèvre L, El Yacoubi S (2020) Social organisation of mobile sensors for wildfire spread estimation. IFAC-PapersOnLine 53(2):3596–3601. https://doi.org/10.1016/j.ifacol.2020.12.2545

Plénet T, El Yacoubi S, Raïevsky C, Lefèvre L (2022) Observability and reconstructibility of bounded cellular automata. Int J Syst Sci. https://doi.org/10.1080/00207721.2022.2064556

Sarachik P, Kreindler E (1965) Controllability and observability of linear discrete-time systems. Int J Control 1(5):419–432. https://doi.org/10.1080/00207176508905497

Urıas J, Salazar G, Ugalde E (1998) Synchronization of cellular automaton pairs. Chaos: Interdiscip J Nonlinear Sci 8(4):814–818. https://doi.org/10.1063/1.166367

Wolfram S (1984) Universality and complexity in cellular automata. Physica D 10(1–2):1–35. https://doi.org/10.1016/0167-2789(84)90245-8

Zhu Q, Liu Y, Lu J, Cao J (2018) Observability of boolean control networks. Sci China Inf Sci 61(9):1–12. https://doi.org/10.1007/s11432-017-9135-4